Thermodynamics of the Relativistic Fermi gas in D Dimensions

Francisco J. Sevilla[a,*], Omar Piña[a]

[a] *Instituto de Física, Universidad Nacional Autónoma de México, Apdo. Postal 20-364, 01000, México D.F., México*

Abstract

The influence of spatial dimensionality and particle-antiparticle pair production on the thermodynamic properties of the relativistic Fermi gas, at finite chemical potential, is studied. Resembling a "phase transition", qualitatively different behaviors of the thermodynamic susceptibilities, namely the isothermal compressibility and the specific heat, are markedly observed at different temperature regimes as function of the system dimensionality and of the rest mass of the particles. A minimum in the temperature dependence of the isothermal compressibility marks a characteristic temperature, in the range of tenths of the Fermi temperature, at which the system transit from a "normal" phase, to a phase where the gas compressibility grows as a power law of the temperature.

1. Introduction

Soon after the discovery of the quantum statistics that incorporates Pauli's exclusion principle [1], by Fermi [2] and Dirac [3], the ideal Fermi gas (IFG) has been extensively used to describe, both qualitatively and quantitatively, many physical phenomena in a wide range of values of the particles density, from cosmological scales to nuclear ones. With the development of atomic trapping and cooling techniques at the end of the 20th century, quantum degeneration of a trapped Fermi gas of ^{40}K atoms [4] was experimentally realized, this achieve-

*Corresponding author
Email address: fjsevilla@fisica.unam.mx (Francisco J. Sevilla)

ment reignited the interest on the theoretical study of the thermodynamical and dynamical properties of the Fermi gas in the weakly interacting regime [5, 6, 7, 8, 9, 10, 11, 12, 13, 14, 15]. More recently, the IFG has been considered in the context of quantum information, where the entanglement entropy of it has been obtained in Ref. [16], while in Ref. [17] exact relations between the Renyi entanglement entropies and the particle number fluctuations in a system of noninteracting fermions have been derived.

On the other hand, Fermi systems at extreme density and/or high temperatures have been of great interest in different fields, from astrophysics to heavy ion collisions, where the physical processes involved are indeed relativistic [18, 19]. Studies of the relativistic IFG in thermal equilibrium have been made over the last quarter of the last century and applied as a simple model system to describe different phenomena, as the stability of white dwarf stars [20], hot quark matter in a giant MIT bag [21], the properties of the gluon-quark plasma [22] which is thought to occurred some microseconds after the Bing-Bang at the early stage of the Universe, etc. [23, 24, 25]. For thermal energies in the nonrelativistic regime it is safe to neglect particle-antiparticle pair production predicted by quantum field theory, thus the only relativistic corrections on the thermodynamics of the IFG to be considered, would correspond to the correct relativistic energy spectrum of a single-particle (for large particle densities, energies around the Fermi energy can be relativistic).

In Refs. [27, 26] P.-H. Chavanis discussed the effects of the spatial dimensionality in the balance between the pressure due to the quantum effects of the electron degeneracy and gravitational collapse due to self-gravitation in white dwarf stars, thus extending the work of Chandrasekhar. In his analysis, the author shows that the collapse or evaporation of the star is unavoidable in dimensions larger than four, and unveils the special character of systems of spatial dimension $d \leq 3$ given by the anthropic principle. The equilibrium properties of the electron gas in the star are rather well approximated by those in the limit of complete quantum degeneration, *i.e.* by those at zero temperature, due to the disparate difference between the system temperature and the Fermi tempera-

ture, whose ratio T/T_F, is in the range $10^{-3} - 10^{-2}$ and thus it is not necessary to consider particle-antiparticle pair production.

Moreover, the effects of low spatial-dimensionality on the non-relativistic IFG at finite temperatures are exhibited in the form of an *unusual* temperature dependence of the chemical potential $\mu(T)$ at constant volume [28, and reference therein]. These effects are markedly shown in an IFG trapped in an impenetrable, one dimensional box potential, for which $\mu(T)$ starts rising quadratically with T above the Fermi energy instead of decreasing from it, as it does in the three-dimensional case. Eventually, at larger temperatures, $\mu(T)$ turns to its usual monotonic decreasing behavior at a characteristic temperature T^* that can be as large as twice the Fermi one. This turn implies a maximum value of μ at T^*, which serves as a characteristic temperature that marks a crossover from a phase ($T < T^*$) at which changes of the Helmholtz free energy is dominated by the internal energy changes, to a "normal" phase ($T > T^*$) at which changes of entropy are the ones that predominantly contribute to the changes of the free energy [29]. In this paper we show the dramatic changes to this picture due to the inclusion of particle-antiparticle pair production.

If thermal energies are relativistic, i.e. $k_B T \sim mc^2$, where m is the rest mass of a single fermion, particle-antiparticle pair production can no be neglected and becomes important as occurs, for instance, in astrophysical plasmas [30, 31, 32]. Though the inclusion of pair production effects on the equilibrium properties of the IFG have been addressed in Refs. [33, 34], the effects of dimensionality has not yet been explored. This contrasts with the case of the relativistic Bose gas, whose thermodynamics has been thoroughly studied considering pair production and dimensionality [37, 36, 38, 39, 35].

In this paper we focus our study on the relativistic effects of particle-antiparticle pair production and spatial dimensionality on the thermodynamic properties of the Fermi gas in the weakly interacting limit. Though, particular attention is paid to the temperature dependence of the chemical potential, which has motivated several discussion of its importance on different levels and contexts [40, 41, 42, 43, 44, 45, 46, 47, 48, 29], our main results focus on the thermody-

namic susceptibilities or response functions, namely the specific heat at constant volume C_V and the isothermal compressibility κ_T, for which there is a great interest at conditions of extreme densities and/or temperatures. Our calculations reveal the appearance of a crossover between qualitatively different behaviors, as function of temperature, of C_V and κ_T due to pair production. Such crossover occurs at a characteristic energy scale corresponding to a thermal energy of a few tenths of the Fermi temperature. This drastic qualitative change in behavior can be plausibly considered as a phase transition, from a normal phase at which the compressibility diminishes with temperature, as in standard fermion systems, to another at which matter becomes arbitrarily compressible.

The paper is organized as follows: In section 2 we describe explicitly the system of our study and the chemical potential is calculated from the principle of charge conservation. In section 3 the isothermal compressibility and the heat capacity at constant volume are calculated. Finally, conclusion and final remarks are given in section 4.

2. Finite temperature: the effects of pair production

The system under consideration corresponds to a d-dimensional gas of non-interacting fermions in thermodynamic equilibrium at finite temperature and chemical potential. Pair production is assumed to occur at thermal equilibrium. At zero temperature the system consists of N_0 spin-$\frac{1}{2}$ fermions (antifermions may be equally chosen instead), of rest mass m in a volume V_d, with single-particle relativistic energy spectrum

$$E_k = \sqrt{c^2\hbar^2k^2 + m^2c^4}, \tag{1}$$

where $\hbar k$ is the momentum of the particle and c is the speed of light. For simplicity we assume the spin balanced case in which the number of fermions in each spin projection $s = \pm\frac{1}{2}\hbar$ are equal, and no spin dependent interactions are considered.

We introduce the ratio $\widetilde{m} = m/m_F$ of the single-particle rest mass to the *Fermi mass* $m_F \equiv \hbar k_F/c$, as the parameter that tunes the system from the

non-relativistic limit, $\widetilde{m} \gg 1$, $E_k \simeq mc^2 + \hbar^2 k^2/2m$, to the ultrarelativistic one $\widetilde{m} \ll 1$, $E_k \simeq \hbar c k$, with the Fermi wavevector k_F defined through the Fermi energy $E_F \equiv \sqrt{c^2\hbar^2 k_F^2 + m^2 c^4}$, that gives the energy of the higher occupied state at zero temperature. In d dimensions the Fermi mass has the following explicit dependence on the fixed, particle density $n_0 = N_0/V$

$$m_F = 2\hbar\pi^{1/2} \left[\Gamma(d/2+1)/2\right]^{1/d} |n_0|^{1/d}/c, \tag{2}$$

which make clear why, for systems of high density, the ultrarelativistic limit corresponds to $\widetilde{m} \ll 1$ for which we have $E_F = E_F^{UR} + \widetilde{m}^2/2 + \ldots$ with $E_F^{UR} = m_F c^2$. In the non-relativistc limit $E_F \simeq mc^2 + E_F^{NR}$, with $E_F^{NR} = \hbar^2 k_F^2/2m$ is the well known non-relativistic Fermi energy.

According to Quantum Field Theory the relativistic effects of pair production are expected to be important at temperatures of the order of mc^2/k_B [35, 49]. At equilibrium, the mixture of particles and antiparticles is taken into account by the condition $\mu = -\bar{\mu}$ [49], which is straightforwardly obtained by the thermodynamical equilibrium condition on the Helmholtz free energy $F(T, V_d, N, \overline{N})$. N and $\overline{N}$ denote the systems's number of particle and antiparticles, respectively, at temperature T and volume V_d. Unless otherwise indicated, we denote with an overbar, those quantities related to antiparticles.

The thermodynamic properties are obtained from the grand partition function

$$\Xi(T, V_d, \mu) \equiv \mathrm{Tr}\left\{\exp\left(-\beta\left[\boldsymbol{H} - \mu(\boldsymbol{N} - \overline{\boldsymbol{N}})\right]\right)\right\}, \tag{3}$$

where $\beta = (k_B T)^{-1}$, k_B is the constant of Boltzmann and Tr denotes the trace over all the states $|n_{\boldsymbol{k}_1,s} n_{\boldsymbol{k}_2,s} \ldots\rangle \otimes |\overline{n}_{\boldsymbol{k}_1,s} \overline{n}_{\boldsymbol{k}_2,s} \ldots\rangle$ in Fock space. $\boldsymbol{k}_i$ denotes the d-dimensional wavevector and s the value of two possible projections of spin. $\boldsymbol{H} = \sum_{\boldsymbol{k},s} E_k \left(\boldsymbol{n}_{\boldsymbol{k},s} + \overline{\boldsymbol{n}}_{\boldsymbol{k},s}\right)$, $\boldsymbol{N} = \sum_{\boldsymbol{k},s} \boldsymbol{n}_{\boldsymbol{k},s}$ and $\overline{\boldsymbol{N}} = \sum_{\boldsymbol{k},s} \overline{\boldsymbol{n}}_{\boldsymbol{k},s}$ denote the Hamiltonian, the total number of particles and a anti-particles operators respectively, in terms of the number operators $\boldsymbol{n}_{\boldsymbol{k},s} = \boldsymbol{a}^\dagger_{\boldsymbol{k},s} \boldsymbol{a}_{\boldsymbol{k},s}$, $\overline{\boldsymbol{n}}_{\boldsymbol{k},s} = \overline{\boldsymbol{a}}^\dagger_{\boldsymbol{k},s} \overline{\boldsymbol{a}}_{\boldsymbol{k},s}$, with eigenvalues $n_{k,s}$, $\overline{n}_{k,s}$, where $\boldsymbol{a}^\dagger_{\boldsymbol{k},s}$ ($\overline{\boldsymbol{a}}^\dagger_{\boldsymbol{k},s}$) and $\boldsymbol{a}_{\boldsymbol{k},s}$ ($\overline{\boldsymbol{a}}_{\boldsymbol{k},s}$) are the creation and annihilation operators of particles (antiparticles), respectively, that satisfy the anti-commutation relations $\left\{\boldsymbol{a}_{\boldsymbol{k}',s'}, \boldsymbol{a}^\dagger_{\boldsymbol{k},s}\right\} = \delta_{\boldsymbol{k},\boldsymbol{k}'}\delta_{s,s'}$, $\left\{\boldsymbol{a}^\dagger_{\boldsymbol{k}',s'}, \boldsymbol{a}^\dagger_{\boldsymbol{k},s}\right\} =$

$\left\{\boldsymbol{a}_{\boldsymbol{k}',s'},\ \boldsymbol{a}_{\boldsymbol{k},s}\right\} = 0$ for particle operators and analogously, $\left\{\overline{\boldsymbol{a}}_{\boldsymbol{k}',s'}, \overline{\boldsymbol{a}}^{\dagger}_{\boldsymbol{k},s}\right\} = \delta_{\boldsymbol{k},\boldsymbol{k}'}\delta_{s,s'}$, $\left\{\overline{\boldsymbol{a}}^{\dagger}_{\boldsymbol{k}',s'}, \overline{\boldsymbol{a}}^{\dagger}_{\boldsymbol{k},s}\right\} = \left\{\overline{\boldsymbol{a}}_{\boldsymbol{k}',s'}, \overline{\boldsymbol{a}}_{\boldsymbol{k},s}\right\} = 0$ for antiparticle ones. The grand canonical partition function results

$$\Xi(T, V_d, \mu) = \prod_{\boldsymbol{k},s} \left(1 + ze^{-\beta E_k}\right)\left(1 + \overline{z}e^{-\beta E_k}\right), \tag{4}$$

with $z = e^{\beta\mu}$, $\overline{z} = z^{-1}$, the fugacity of particles and antiparticles, respectively. From this, we have that

$$\ln \Xi(T, V_d, \mu) = \sum_{\boldsymbol{k},s} \left[\ln\left(1 + ze^{-\beta E_k}\right) + \ln\left(1 + z^{-1}e^{-\beta E_k}\right)\right]. \tag{5}$$

The net number of particles in the system at T y V_d is given by

$$\begin{aligned} N - \overline{N} &= \left[z\frac{\partial \ln \Xi}{\partial z}\right]_{T,V_d} \\ &\equiv \sum_{\boldsymbol{k},s} \left[\langle n_{E_k}\rangle - \langle \bar{n}_{E_k}\rangle\right], \end{aligned} \tag{6}$$

where $\langle n_{E_k}\rangle = \{\exp\left[\beta(E_k - \mu)\right] + 1\}^{-1}$ and $\langle \bar{n}_{E_k}\rangle = \{\exp\left[\beta(E_k + \mu)\right] + 1\}^{-1}$ give, respectively, the average number of fermions and anti-fermions in the energy state E_k. This equation relates the chemical potential of the system to the initial density of particles $n_0 = N_0/V_d$, where $N_0 = (N - \overline{N})$ is a conserved quantity. In the limit of the continuum we have

$$n_0 = R_d \int_0^{\infty} dk\, k^{d-1} \left[\langle n_{E_k}\rangle - \langle \bar{n}_{E_k}\rangle\right], \tag{7}$$

where $R_d \equiv 4\pi^{d/2}/[(2\pi)^d \Gamma(d/2)]$ is a constant that depends only on d. Expression (7) can be written in terms of hyperbolic functions as

$$n_0 = R_d \int_0^{\infty} dk\, k^{d-1} \frac{\sinh \beta\mu}{\cosh \beta E_k + \cosh \beta\mu} \tag{8}$$

and simplifies to

$$n_0 = -\frac{R_d \Gamma(d)}{(\beta\hbar c)^d}\left[\mathrm{Li}_d\left(-z\right) - \mathrm{Li}_d\left(-z^{-1}\right)\right] \tag{9}$$

in the ultrarelativistic limit and to

$$n_0 = \frac{R_d \Gamma(d/2)}{2(\beta\hbar^2/2m)^{d/2}}\left[-\mathrm{Li}_{d/2}\left(-z^{NR}\right)\right] \tag{10}$$

in the non-relativistic one, with $z^{NR} \equiv e^{\beta\mu^{NR}}$ the non-relativistic fugacity and $\mu^{NR} \equiv \mu - mc^2$. In the last expressions $-\mathrm{Li}_\sigma(-z) \equiv [1/\Gamma(\sigma)] \int_0^\infty dx\, x^{\sigma-1}/[e^x z^{-1} + 1]$ is the polylogarithm function, which has the series representation $-\sum_{l=1}^{\infty}(-z)^l/l^\sigma$ for $|z| < 1$.

In the ultra-relativistic regime, equations (9) and (18) (see below), involve expressions of the kind $\left[-\mathrm{Li}_n(-z) - (-1)^n \mathrm{Li}_n\left(-z^{-1}\right)\right]$, which can be written in terms of a polynomial of degree n in $(\beta\mu)$ by the use of the Bernoulli polynomials, $\mathrm{B}_n(x) = \sum_{k=0}^{n} \binom{n}{k} b_{n-k}\, x^n$ [50], as $[(2\pi i)^n/n!]\, \mathrm{B}_n(1/2 + \beta\mu/2\pi i)$, where the b_k's are the Bernoulli numbers [51], the first ones being $b_0 = 1$, $b_1 = -1/2$, $b_2 = 1/6$, $b_3 = 0 \ldots$ Thus, for odd d, expression (9) can be written as a polynomial in odd powers of $\beta\mu$ as

$$n_0 = \frac{R_d \Gamma(d)}{(\beta\hbar c)^d} \sum_{j\,\mathrm{odd}}^{d} \frac{(\beta\mu)^j}{j!} \eta_{d,j}, \tag{11}$$

where the coefficients $\eta_{n,m}$ are given explicitly by

$$\eta_{n,m} = (2\pi i)^{n-m} \sum_{k=m}^{n} \frac{b_{n-m}}{2^{k-m}(n-k)!(k-m)!}. \tag{12}$$

The coefficients are real quantities since n and m are odd integers. We have then that in the ultra-relativistic regime, $\mu = m_F c^2$ for $d = 1$.

2.1. The chemical potential

Before discussing the temperature dependence of μ in the regime of interest, we comment in passing that at low enough temperatures, when pair production is negligible, application of the commonly used Sommerfeld expansion [52] to Eq. (7), gives for the chemical potential

$$\frac{\mu(T)}{E_F} = 1 - \frac{\pi^2}{6}\left(\frac{T}{T_F}\right)^2 \left[1 + (d-2)(1+\widetilde{m}^2)\right], \tag{13}$$

where the sign in front of the factor $(T/T_F)^2$ depends explicitly on $\widetilde{m}$. From this expression, a simple analysis shows that a *non-monotonic* dependence on T is possible whenever the dimensionality of the system is strictly smaller than $2 - \left(1 + \widetilde{m}^2\right)^{-1}$. This inequality generalizes the one reported in Refs. [28, 29], in that incorporates the effects of finite rest mass, and reduces to the

$\widetilde{m}-$independent inequalities $d < 1$ and $d < 2$, in the ultrarelativistic and non-relativistic limit respectively. These two values for d correspond to the values for which the IFG is thermodynamically equivalent—in that the specific heat has the same temperature dependence—to the ideal Bose gas.

In Fig.1(a), $\mu(T)$ is shown as function of T for the case when pair production is neglected (dashed lines), for dimensions 1/2, 1 ,2, 3 and 4; and for $\widetilde{m} = 1$. In this situation, the non-monotonous behavior is exhibited as a local maximum for $d = 1/2$ (first dashed line from the far right) and for $d = 1$ (second dashed line from the far right). The appearance of maxima persist only for systems with $d < 1$ in the ultrarelativistic regime $\widetilde{m} \to 0$. On the contrary, when $\widetilde{m}$ is increased, the non-monotonic behavior of $\mu(T)$ is expected for systems with $d < 2$ if pair production is neglected (dashed lines in Fig.1(b), the expected maxima for $d < 2$ are not revealed in the figure since the exact E_F has been chosen as energy scale, however, if E_F^{NR} is chosen as energy scale we recover the non-monotonic behavior of the non-relativistic IFG $\mu^{NR} = \mu - mc^2$ as shown in Refs. [28, 29]).

In the high temperature regime, without pair production, $\mu(T)$ is given by

$$-k_B T \ln\left[\frac{V_d}{N\lambda^d}\, 2\left(\frac{2\pi k_B T}{mc^2}\right)^{(d-1)/2} K_{(d+1)/2}\left(\frac{mc^2}{k_B T}\right)\right],$$

where $\lambda = h/mc$ is the Compton wavelength and $K_\nu(z)$ denotes the Bessel function of the second kind of order ν. Last expression corresponds to the classical result for which the chemical potential is negative and decreases monotonically with temperature (see dashed lines in Fig. 1). In addition, the same expression is also obtained for N spinless relativistic bosons of mass m in the same limit [37]. This trivial relationship between the Bose and Fermi gas is simply established by the loss of quantum degeneracy due to thermal fluctuations.

Effects of pair production.. By solving Eq. (7) at constant volume, we show that the combined effects of pair production and system dimensionality are conspicuous on the temperature dependence of $\mu(V_d, T)$ as is shown in Fig. 1 (solid lines with symbols).

We focus in the high temperature regime, for which the chemical potential has three distinct asymptotic limits: i) it goes to zero if $d > 1$; ii) it goes to the constant value $E_F \left[1 + \widetilde{m}^2\right]^{-1/2}$ if $d = 1$ and iii) diverge sub-linearly as a power law for $0 < d < 1$. These behaviors are accounted for by the expression

$$\mu(T) \sim E_F \left(\frac{T}{T_F}\right)^{1-d} \Phi(\widetilde{m}^2 + 1, d), \tag{14}$$

which is approximately obtained from Eq. (7), with $\Phi(\xi, d)$ a temperature-independent quantity defined through the expression

$$[\Phi(\xi, d)]^{-1} = d \int_0^\infty dx\, x^{d-1} \left[1 + \cosh\left(\frac{x^2}{\xi}\right)^{1/2}\right]^{-1}. \tag{15}$$

In Table 1 explicit functional forms for $[\Phi(\xi, d)]^{-1}$ are given for $d = 4$, 3, 2 and 1.

Table 1: Explicit functional forms for $[\Phi(\xi, d)]^{-1}$ which appears in eq. (14).

	$d = 4$	$d = 3$	$d = 2$	$d = 1$
$\Phi(\xi, d)^{-1}$	$36\,\xi^2\,\zeta(3)$	$\pi^2\,\xi^{3/2}$	$2\,\xi\,\ln 4$	$\xi^{1/2}$

In the ultrarelativistic limit, the explicit dependence on temperature can be obtained for odd dimensions, namely $\mu(T)/E_F = 1$ for $d = 1$, and

$$\frac{\mu}{E_F} = \left[\frac{1}{2} + \sqrt{\left(\frac{\pi}{\sqrt{3}}\frac{T}{T_F}\right)^6 + \frac{1}{4}}\right]^{1/3} + \left[\frac{1}{2} - \sqrt{\left(\frac{\pi}{\sqrt{3}}\frac{T}{T_F}\right)^6 + \frac{1}{4}}\right]^{1/3} \tag{16}$$

for the three-dimensional case [21]. In Fig.1 $\mu(T)$ is shown for the mass ratio $\widetilde{m} = 1$ [panel (a)] and $\widetilde{m} = 100$ [panel (b)]. In both cases, the solid-red line with squares, which corresponds to $d = 1$, marks the division from the two different behaviors i) and iii).

The effects of pair production on the chemical potential are puzzling for $d < 1$, for it makes μ to grow monotonically for all temperature if $d < 1$ and $\widetilde{m} \lesssim 2$. Though, thermodynamics at these dimensions would seem out of place,

the limit $d \to 0$ has been analyzed in Ref. [53] for the non-relativistic IFG, giving a physically consistent interpretation on the meaning of the large values of the chemical potential as $d \to 0$ [54]. On the other hand, effective low dimensions do occur in trapped systems [55, 56, 29], where the trapped system is mapped into a free one but in an effective dimension that is related directly to the density of states. The monotonic growing of μ with T for $d < 1$ can be understood qualitatively in the same line of thought as in Ref. [29]: as the system temperature is increased so is the number of particles and anti-particles in the system, in fact pair production for $d < 1$ increases with T at a more low rate than for larger dimension (see Fig. 2), thus anti-particles can be neglected. It is then plausible to assume that the average number of particles in state E_k, $\langle n_{E_k} \rangle$, be larger than 1/2, which requires μ to be larger than the Fermi energy, since the number of particles increases monotonically with temperature, this growing behavior is expected to happen for all T. These considerations make clear why the system at high temperature behaves quite differently from the classical gas counterpart for which $\langle n_{E_k} \rangle \ll 1$. As the ratio $\widetilde{m}$ is increased above 4, approximately, this last behavior is changed, the chemical potential goes from a decreasing behavior to an increasing one as can be noticed in Fig. 1(b) for $\widetilde{m} = 100$.

For $d > 1$, the effects of the original number of particles are outweighed by pair production, reaching the limit $N \approx \overline{N}$ as temperature is increased (see Fig. 2). This results emerge from the dependence on T of μ, which goes to zero as T^{1-d}, this implies $z \to \overline{z}$. The particular dependence of μ on T, for different dimensions and values of $\widetilde{m}$, leads to different particle-antiparticle pair production rate as is exhibited in Fig.2, where the ratio of the antiparticles number to the particles number, $\overline{N}/N$, is shown as function of temperature for $\widetilde{m} = 1$. In the inset, the effects of disparate masses, namely $\widetilde{m} = 0.01$, 1, 100, are shown for $d = 3$.

3. Thermodynamic susceptibilities

It is well known that the thermodynamic susceptibilities play an important role in equilibrium transformations, such as the cooling by adiabatic compression or by an isocoric transformation of a gas, in such cases, the constant volume specific heat C_V and the isothermal compressibility κ_T are of particular importance. On the one hand, it has been suggested in Ref. [29], on the grounds of an energy-entropy argument, that the non-monotonic behavior of the chemical potential of the nonrelativist IFG, indicates a crossover from an unconventional equilibrium states to standard states of the IFG.

For the non-relativistic IFG, these susceptibilities show a monotonic behavior as function of T for dimensions $d \geq 2$ [28]. C_V shows a "hump" for $d < 2$ that is directly related to the non-monotonic behavior of $\mu(T)$ and means that, for low dimensional systems, the IFG dissipate thermal fluctuations more effectively in the temperature region where $\mu(T) > E_F$. On the other hand, the isothermal compressibility also exhibits a "hump" for $d < 2$ with a maximum at a characteristic temperature T_κ [29]. For $T > T_\kappa$ the system compressibility diminish, vanishing as the temperature goes to infinity just like the ideal classical gas, however, below T_κ, the compressibility of the gas rises with T above its value at zero temperature, κ_0 [see Eq. (A.13) in the appendix], the gas turns to be more compressible than the $T = 0$ state. In addition, a thermodynamic "equivalence" between the ideal Bose and Fermi gases in $d = 2$ has been analyzed [57, 58] and extended to a more general energy-momentum dispersion relation [59]. Such equivalence is understood as the fact that both gases have the same temperature dependence of their respective specific heat at constant volume.

Now we turn to analyze the effects of pair production on κ_T and C_V of the relativistic IFG. A quantity of interest that is relevant in the study of fluctuations corresponds to $\Lambda_{E_k} \equiv \langle n_{E_k} \rangle (1 - \langle n_{E_k} \rangle)$, which gives account of the variance of the occupation number of particles in the energy-state E_k. The dependence on β and μ has not been made explicit for the economy of writing, however, it is clear that for a given value of T, Λ_E is obtained after substitution

of the corresponding value of μ computed from Eq. (7). In Fig. 3 we present Λ_E and its counterpart for antiparticles $\overline{\Lambda}_E$, as function of E, for $d = 3$, $\widetilde{m} = 1$, and for temperatures at which: a) pair production is negligible $T/T_F = 0.1$ (circles) for which Λ_E varies around the Fermi energy as expected, while $\overline{\Lambda}_E \simeq 0$; b) pair production starts rising $T/T_F = 0.3$ (triangles); and c) $T/T_F = 0.7$ where antiparticles almost equals the particles number (squares).

3.1. The isothermal compressibility κ_T

The isothermal compressibility is worth of analysis since is directly related to the number fluctuations of the system and such quantity can be used to characterize many situations of the IFG, as entanglement of the IFG [17], for instance.

At finite temperature, κ_T can be computed from the expression $(1/n_0^2)\left(\partial n_0/\partial\mu\right)_T$ which results, after the use of expression (7), into

$$\kappa_T = \frac{R_d}{n_0^2 k_B T}\int_0^\infty dk\, k^{d-1}\left[\Lambda_{E_k} + \overline{\Lambda}_{E_k}\right]. \tag{17}$$

In the ultrarelativistic limit, last expression simplifies in terms of polylogarithm functions to

$$\kappa_T = \frac{R_d\Gamma(d)}{n_0^2(\hbar c)^d}(k_B T)^{d-1}\left[-\mathrm{Li}_{d-1}(-z) - \mathrm{Li}_{d-1}(-z^{-1})\right] \tag{18}$$

and to

$$\kappa_T = -\frac{R_d\Gamma(d/2)}{n_0^2\left(\hbar^2/2m\right)^{d/2-1}}(k_B T)^{d/2-1}\mathrm{Li}_{d/2-1}(-z^{NR}) \tag{19}$$

in the non-relativistic one.

Expression (18) can be written as an even polynomial of order $d-1$ in $\beta\mu$, namely

$$\kappa_T = \frac{R_d\Gamma(d)}{n_0^2(\hbar c)^d}(k_B T)^{d-1}\sum_{j\,\mathrm{even}}^{d-1}\frac{(\beta\mu)^j}{j!}\eta_{d,j}, \tag{20}$$

where the coefficients $\eta_{l,n}$ are given in equation (12). For $d = 1$ it can be checked straightforwardly that $\kappa_T = (\pi/2)\hbar c/m_F^2 c^4 = \kappa_0$, i.e, in the ultra-relativistic regime, the isothermal compressibility remains at its value at $T = 0$ for all T as effect of pair creation.

In Fig. 4, κ_T is shown as function of temperature for: $\widetilde{m} = 1$ [relativistic case, panel (a)] and $\widetilde{m} = 100$ [non-relativistic case, panel (b)] and $d = 1/2$, 1, 2, 3, and 4 in each case. The ultrarelativistic limit $\widetilde{m} \ll 1$, has been omitted since analytical expression have been obtained. In the low temperature regime and for values of d and $\widetilde{m}$, to be determined, the compressibility rises and eventually starts diminishing with temperature exhibiting a maximum at T_κ. A calculation based on the observation that the product $\langle n_E \rangle (1 - \langle n_E \rangle)$ is different from zero only in a narrow interval of energies around μ (see Fig. 3 for $T/T_F = 0.01$) gives, up to second order terms in T/T_F,

$$\kappa_T \simeq \frac{d\mu \left(\mu^2 - m^2c^4\right)^{d/2-1}}{n_0 (m_F c^2)^d} \left(1 + \frac{\pi^2}{6} \left(k_B T\right)^2 (d-2) \times \right.$$
$$\left. \left(\mu^2 - m^2c^4\right)^{-2} \left[3\left(\mu^2 - m^2c^4\right) + (d-4)\mu^2\right]\right) \quad (21)$$

and by using Eq. (13) we have that

$$\frac{\kappa_T}{\kappa_0} \simeq 1 - \frac{\pi^2}{6} \left(\frac{T}{T_F}\right)^2 \left[1 - 2(d-2)(1+\widetilde{m}^2) - \right.$$
$$\left. (d-2)(d-4)(1+\widetilde{m}^2)^2\right], \quad (22)$$

which shows the nonmonotonic dependence with temperature whenever

$$d < \frac{2 + 3\widetilde{m}^2 - \left(1 + \widetilde{m}^4\right)^{1/2}}{(1+\widetilde{m}^2)}. \quad (23)$$

This raising of the compressibility with temperature is an abnormal feature that would have important effects on some thermodynamical transformations in low dimensional systems at low temperatures [60, 61].

In the ultrarelativistic limit, $\widetilde{m} \ll 1$, such abnormal behavior is presented for systems in dimensions smaller than 1, as can be checked from the expression

$$\frac{\kappa_T}{\kappa_0} = 1 + \frac{\pi^2}{6}(d-1)(d-2) \left(\frac{T}{T_F}\right)^2 \quad (24)$$

or directly from (23). For $d = 1$, κ_T becomes temperature independent as can be checked straightforwardly from expression (18) getting the value $\kappa_0^{UR} = \left(\pi \hbar c\, n_0^2\right)^{-1}$ [see Eq. (A.15) in the Appendix]. Note that for the case $d = 2$, κ_T

is proportional to μ, which turns to be a monotonic decreasing function of T for any value of $\widetilde{m}$. In the regime $\widetilde{m} \gg 1$, condition (23) turns simply into $d < 2$ [29] .

As temperature is increased and pair production becomes important, κ_T suffers a *striking change* in its temperature dependence when $d > 1$, namely, instead of diminishing to zero as occurs if pair creation is neglected (dashed lines in Fig. 4), it starts to rapidly grow with temperature. This behavior is set on when the number of antiparticles is of the order of particles, and is marked by a local minimum T^*_κ in the range of the tenths of the Fermi temperature. At higher temperatures, κ_T grows with T asymptotically as

$$\kappa_0 \left(1+\widetilde{m}^2\right)^{d/2-1} (d-1)!\, \zeta(d-1)\, 2\left(1-2^{2-d}\right) \left(\frac{T}{T_F}\right)^{d-1},$$

with $\zeta(x)$ the Riemann zeta function.

This drastic change of the temperature dependence of κ_T is not only quantitative, but *qualitative* in essence, the equilibrium properties of the system, driven by pair production at equilibrium, transit from a *normal phase* (in that show standard behavior of the thermodynamic properties), to a phase in which the system becomes arbitrarily compressible with temperature, as occurs in the relativistic Bose gas. For the three-dimensional case we have that the minimum of κ_T occurs at approximately at $T^*_\kappa = 0.34732$ for $\widetilde{m} = 0.01$, $T^*_\kappa = 0.32018$ for $\widetilde{m} = 1$, and $T^*_\kappa = 0.07465$ for $\widetilde{m} = 100$.

In small particle densities systems, as those occurring in dwarf white stars (10^{-9} electrons per fm^{-3}), the temperatures needed to observe the transition would be two orders of magnitude larger than the ones in the star core. However at particle densities of the order of the nuclear matter 0.122 fm^{-3}, the corresponding Fermi energy is approximately 480.618 MeV in the limit $\widetilde{m} \ll 1$. With these values we estimate $k_B T^*_\kappa \simeq 166.928$ MeV for $\widetilde{m} = 0.01$. This value is of the order of the expected crossover temperature to the quark-gluon plasma [62], which from QCD calculations is expected to be 173$\pm$15 MeV for massless quarks [63].

In contrast, κ_T/κ_0 tends asymptotically with temperature to the constant

value $(1+\widetilde{m})^{-1/2}$ for $d=1$, while it goes to zero for $d<1$ as can be seen from Fig. 4 for $d=1/2$. In this latter case, though the system behave qualitatively as standard matter, the effects due to pair creation can be noted quantitatively from the departure to the case when no pair creation is considered (thin-dashed lines).

3.2. The specific heat at constant volume C_V

The specific heat at constant volume is expressed in terms of the Λ_{E_k}'s as

$$C_V = \frac{R_d V_d}{k_B T^2}\int_0^\infty dk\, k^{d-1} E_k^2 \left[\Lambda_{E_k}+\overline{\Lambda}_{E_k}\right] - \frac{V_d}{\kappa_T T}\left[\frac{R_d}{n_0 k_B T}\int_0^\infty dk\, k^{d-1} E_k \left[\Lambda_{E_k}+\overline{\Lambda}_{E_k}\right]\right]^2 . \tag{25}$$

As shown in Fig. 5, the low temperature behavior is given by the well known linear dependence, with the prefactor $d\pi^2(1+\widetilde{m}^2)/3$ which comes only from the Fermi-Dirac statistics of the particles and the dimensionality of the system.

In the same range of temperatures where a local minimum in κ_T is found, the specific heat changes its linear dependence characteristic of the low temperature regime, to the temperature dependence T^d as is shown in Fig. 5. For $\widetilde{m} \ll 1$ (not shown in Fig. 5) the transition is smooth and becomes more marked as the mass ratio increases, as is contrasted in panels (a) and (b), where a plateau appears before the power-law growth. This behavior differs from the case for which only particles are considered (thin-dashed lines) which reaches the Dulong-Pettit limit $C_V/dNk_B = 1$. The exact result $C_V/N_0k_B = \left(\pi^2/3\right)(T/T_F)$ is found in the limit $\widetilde{m}\to 0$ for $d=1$.

In Ref. [65] the authors considered the relativistic Bose and Fermi gases, at low temperatures, they rightly neglected the antiparticles, and concluded that in two dimensions both gases are thermodynamically inequivalent, in contrast to the non-relativistic case in which they do, however it seems they missed that both gases are thermodynamically equivalent in one dimension in the ultrarelativistic limit. In fact, it is known that the condition for the equivalence between the two quantum gases consists of the constancy of the single-particle density of states $g(E)$. In the exact relativistic case, is the finite rest mass of the particle what avoids such possibility, since there is no value of d which makes the density

of states $g(E) = E(E^2 - m^2c^4)^{d/2-1}\theta(E - mc^2)$, $\theta(x)$ being the Heaviside step function, to be a constant as occurs in the non-relativistic and ultrarelativistic cases, where $g(E) \propto E^{d/2-1}$ and $\propto E^{d-1}$, respectively.

4. Conclusions and final remarks

We have studied the effects of the system dimensionality and quantum-relativity on the thermodynamics of an ideal Fermi gas. The temperature dependence of the chemical potential is determined by the system dimensionality and by the particles rest mass. We recovered the unusual low temperature dependence of $\mu(T)$ for $d < 2$ [28] in the non-relativistic limit $m \gg m_F$. For arbitrary values of the rest mass, the nonmonotonic behavior of μ in the low temperature regime appears if $d < 2 - (1 + \widetilde{m}^2)^{-1}$, which includes the ultrarelativistic case for $\widetilde{m} \ll 1$. Singularly, for dimensions smaller than one, μ increases monotonically with T. This peculiar behavior occurs since for low dimensional systems, the creation of particle-antiparticle pairs occurs at a so low rate that the initial number of fermions dominates the thermodynamic behavior of the system. This argument is supported from the temperature dependence of κ_T which vanishes as $T \to \infty$, just as in the case when only particles are considered (dashed lines in Fig.1). The temperature dependence of μ for high temperatures described in Fig.1(a) is also observed in the relativistic Bose gas with pair production [37] for $d > 1$, with the remarkable difference that for the Bose gas, $|\mu_B| \leq mc^2$, and therefore the chemical potential vanishes as $T \to \infty$ even for $0 < d < 1$. Except in the case $d = 1$ for which we have $\mu_B = 0$ for all T where μ_B is the chemical potential of the Bose gas.

The effects of pair production are exhibited in the thermodynamical susceptibilities as a change in their temperature dependence that appears at some tenths of the Fermi temperature (as shown in Figs. 4 and 5) corresponding to the temperature range at which the pair production becomes significantly important. Both susceptibilities start growing without limit as a power law of T after this crossover. The temperature that points out the crossover T_κ^* could

be determined from the apparent local minimum exhibited in the isothermal compressibility.

Our calculations consider the exact thermal behavior of the relativistic IFG and therefore can describe systems beyond the standard, complete-degeneracy approximation ($T = 0$), generally used in situations where a disparate difference between the system's and Fermi temperature exists.

5. Acknowledgments

The authors acknowledge financial support from DGAPA-UNAM grant PAPIIT-IN113114.

Appendix A. The zero temperature relativistic IFG

The zero point energy per particle, $u_0 = U_0/N_0$, can be written in terms of the Gaussian or ordinary hypergeometric function ${}_2F_1(a_1, a_2; b_1; z)$ [66] as

$$u_0 = mc^2 \, {}_2F_1\left[-1/2, d/2; 1 + d/2; -\widetilde{m}^{-2}\right]. \tag{A.1}$$

that reduces to elementary functions for integer values of d. For $\widetilde{m} \gg 1$ we have

$$u_0 = mc^2 + \frac{d/2}{1 + d/2} E_F^{NR} - \frac{d/2}{2 + d/2} \frac{\left(E_F^{NR}\right)^2}{mc^2} + \ldots \tag{A.2}$$

In the opposite limit, $\widetilde{m} \ll 1$, we can write

$$u_0 = \frac{d}{d+1} E_F^{UR} \left[1 + \frac{1}{2}\frac{d+1}{d-1}\widetilde{m}^2 - \frac{1}{8}\frac{d+1}{d-3}\widetilde{m}^4 + \ldots\right] \tag{A.3}$$

for $d \neq 1, 3, 5 \ldots$.

For $d = 3$ and 1 we have, respectively

$$u_0 = \frac{3}{4} E_F^{UR} (1 + \widetilde{m}^2)^{1/2} \left[1 + \frac{\widetilde{m}^2}{2}\left(1 - \frac{\widetilde{m}^2 \operatorname{arcsinh}(\widetilde{m}^{-1})}{(1 + \widetilde{m}^2)^{1/2}}\right)\right] \tag{A.4}$$

$$u_0 = \frac{1}{2} E_F^{UR} \left[(1 + \widetilde{m}^2)^{1/2} + \widetilde{m}^2 \operatorname{arcsinh}(\widetilde{m}^{-1})\right], \tag{A.5}$$

In the $\widetilde{m} \ll 1$ limit, last expressions can approximated by

$$u_0 = \frac{3}{4} E_F^{UR} \left[1 + \widetilde{m}^2 + \frac{1}{8}\widetilde{m}^4 \ln(\widetilde{m}) + \ldots\right] \tag{A.6}$$

$$u_0 = \frac{1}{2} E_F^{UR} \left[1 - \widetilde{m}^2 \ln \widetilde{m} + \frac{1}{8}\widetilde{m}^4 + \ldots\right]. \tag{A.7}$$

For the zero point pressure P_0 we have

$$P_0/n_0 = m_F c^2 \sqrt{1+\widetilde{m}^2} - u_0 \tag{A.8}$$

which for $\widetilde{m} \gg 1$ last expression reduces to

$$P_0/n_0 = \frac{2}{d+2} E_F^{NR} + \frac{d/2}{2+d/2} \frac{\left(E_F^{NR}\right)^2}{mc^2} + \dots \tag{A.9}$$

where the first term corresponds to the well known non-relativistic case. In the opposite limit

$$P_0/n_0 = \frac{1}{d+1} E_F^{UR} - \frac{1}{2(d-1)} E_F^{UR} \widetilde{m}^2 + \frac{d}{8(d-1)} E_F^{UR} \widetilde{m}^4 \dots \tag{A.10}$$

the first term corresponds to the well known result in the ultrarelativistic case, the next terms are valid always that d is not an odd integer. For $d = 3, 1$ we have respectively

$$P_0/n_0 = \frac{1}{4} E_F^{UR} - \frac{1}{4} E_F^{UR} \widetilde{m}^2 + \frac{3}{2^5} E_F^{UR} \widetilde{m}^4 \ln \widetilde{m} \dots \tag{A.11}$$

$$P_0/n_0 = \frac{1}{2} E_F^{UR} + \frac{1}{2} E_F^{UR} \widetilde{m}^2 \left[1 - \ln \widetilde{m}\right] - \frac{1}{2^4} E_F^{UR} \widetilde{m}^4 + \dots \tag{A.12}$$

The inverse of the isothermal compressibility $\kappa_T = -\left(1/V_d\right)\left(\partial V_d/\partial P_0\right)_T$ is given by

$$\kappa_0^{-1} = \frac{n_0}{d} \frac{m_F c^2}{\sqrt{1+\widetilde{m}^2}} \tag{A.13}$$

in the limit of $\widetilde{m} \gg 1$ we have that

$$\kappa_0 \simeq \kappa_0^{NR} \left[1 + \frac{1}{2\widetilde{m}^2}\right] \tag{A.14}$$

where $\kappa_0^{NR} = d/[(d+2)P_0]$ is the NR isothermal compressibility, which reduces to the well known result $\kappa_0 = (3/5)P_0^{-1}$ for $d = 3$, and

$$\kappa_0 \simeq \kappa_0^{UR} \left[1 + \frac{1}{2}\widetilde{m}^2\right] \tag{A.15}$$

in the $\widetilde{m} \ll 1$ case, where $\kappa_0^{UR} = d/[(d+1)P_0]$. These results show that the gas is more compressible than in their respective limits $\widetilde{m} \to \infty$ and $\widetilde{m} = 0$.

[1] W. Pauli, Zeitschrift für Physik **31**, 765-83 (1925).

[2] E. Fermi, Rend. Acc. Lincei **3**, 145 (1926).

[3] P. Dirac, Proc. R. Soc. A **112**, 661 (1926).

[4] B. DeMarco, and D. Jin, "Onset of Fermi Degeneracy in a Trapped Atomic Gas," Science **285**, 1703-1706 (1999).

[5] P. Vignolo, A. Minguzzi, and M. P. Tosi, Phys. Rev. Lett. **85**, 2850 (2000).

[6] F. Gleisberg, W. Wonneberger, U. Schlöder and C. Zimmermann, Phys. Rev. A **62**, 063602 (2000).

[7] M.N. Tran, M.V.N. Murthy, and R.K. Bhaduri, Phys. Rev. E **63**, 031105 (2001).

[8] Z. Akdeniz, P. Vignolo, A. Minguzzi, and M.P. Tosi,Phys. Rev. A **66**, 055601 (2002)

[9] P. Vignolo and A. Minguzzi, Phys. Rev. A **67**, 053601 (2003).

[10] D-V Anghel, J. Phys. A: Math. Gen. **36**, L577-L783 (2003).

[11] M.N. Tran, J. Phys. A: Math. Gen. **36**, 961 (2003).

[12] B.P. van Zyl, R.K. Bhaduri, A. Suzuki and M. Brack, Phys. Rev. A **67**, 023609 (2003).

[13] E.J. Mueller, Phys. Rev. Lett. **93**, 190404 (2004)

[14] D. Anghel, O. Fefelov, and Y.M. Galperin, J. Phys. A: Math. Gen **38**, 9405 (2005).

[15] Dae-Yup Song, Phys. Rev. A **74**, 051602(R) (2006).

[16] Dimitri Gioev, and Israel Klich, Phys. Rev. Lett. **96**, 100503 (2006).

[17] Pasquale Calabrese, Mihail Mintchev, Ettore Vicari, Eur. Phys. Lett. **98**, 20003 (2012).

[18] R. Stock, Nature **337**, 319-324 (1989).

[19] Hakim, Rémi. Introduction to Relativistic Statistical Mechanics: Classical and Quantum. World scientific, 2011.

[20] Chandrasekhar, S. 1931, Astrophysical J., 74, 81.

[21] H.-T. Elze, W. Greiner and Johann Rafelski, J. Phys. G: Nucl. Phys. **6** L-149-L153 (1980).

[22] H, Satz, Nature **324**, 116-120 (1986).

[23] S.R. Hore, N.E. Frankel, Phys. Rev. A, **12**, (4) 1617 (1975)

[24] J. Dunning-Davies, J. Phys. A: Math. Gen. **14**, 3005-3012 (1981).

[25] I.A. Howard and N.H. March, J. Phys. A: Math. Gen. **37** 965-971 (2004).

[26] P.-H. Chavanis, Phys Rev. D **76** (2), 023004 (2007).

[27] P.-H. Chavanis, Phys. Rev. E **69** (6), 066126 (2004)

[28] M. Grether, M. de Llano, and M.A. Solís, Eur. Phys. J. D **25**, 287-291 (2003). **44**, 2, Pages 394-399 (2011).

[29] Francisco J. Sevilla, Journal of Thermodynamics, vol. 2017, Article ID 3060348, 12 pages, 2017. doi:10.1155/2017/3060348

[30] A. P. Lightman, 1982, Astrophysical J., **253**, 842

[31] R. Svensson, 1982, Astrophysical J., **258**, 335

[32] R. Ruffini, G. Vereshchagin, S.-S. Xue, Phys. Reps. **487** 1–140 (2010).

[33] S. Cai, G. Su and J. Chen, Int. J. Mod. Phys. B **24**, No. 29, 5783–5792 (2010).

[34] G. Su, L. Chen and J. Chen, Mod. Phys. Lett. B **27**, No. 24, 1350177 (2013).

[35] H.E. Haber & H.A. Weldon, Phys. Rev. Lett. **46**, 1497 (1981).

[36] Surjit Singh and P. N. Pandita, Phys. Rev. A **28**, 1752 (1983).

[37] H. O. Frota, Melquisedech S. Silva and S. Goulart Rosa, Jr, Phys. Rev. A **39** (2), 830-834 (1989).

[38] M. Grether, M. de Llano, and George A. Baker Jr. Phys. Rev. Lett. **99**, 20, 200406 (2007).

[39] G. Su, L. Chen, and J. Chen. J. Phys. A: Math. Theor. **41**, 28, 285002 (2008).

[40] G. Cook & R.H. Dickerson, Am. J. Phys. **63** (8), 737-742 (1995).

[41] R. Baierlein, Am. J. Phys. **69** (4), 423-434 (2001).

[42] G. Job and F. Herrmann, Eur. J. Phys. **27**, 353-371 (2006).

[43] Carl E. Mungan, Eur. J. Phys. **30**, 1131-1136 (2009).

[44] M.R.A. Shegelski, Solid State Commun. **58**, 351-354 (1986);

[45] P.T. Landsberg and D.C. Browne, Solid State Commun. **62**, 207-208 (1987);

[46] M.R.A. Shegelski, Am. J. Phys. **72**, 676-678 (2004);

[47] T.A. Kaplan, J. Stat. Phys. **122**, 1237-1260 (2006).

[48] F.J. Sevilla and L. Olivares-Quiroz, Eur. J. Phys., **33** (3), 709 (2012).

[49] Huang, Kerson. Introduction to statistical physics. CRC Press, 2001.

[50] A. Erdélyi, W. Magnus, F. Oberhettinger, F.G. Tricomi *Higher Transcendental Functions*, Vol. 1 (Malabar, FL: R.E. Krieger Publishing) (1981).

[51] L. Carlitz, Fibonacci Quarterly, 6: 71–85 (1968).

[52] N. W. Ashcroft, N. D. Mermin *Solid State Physics*, (Harcout College Publishers,1976) p. 826.

[53] M.H. Lee, Phys. Rev. E **54** (1), 946 (1996).

[54] I. Chávez, M. Grether, and M. de Llano, Physica E

[55] B. Vanderlei, D.E. Pritchard, and D. Kleppner Phys. Rev. A **35**, 4354 (1987).

[56] V. Bagnato and D. Kleppner Phys. Rev. A **44**, 7439 (1991).

[57] Robert M. May, Phys. Rev. **135** (6A), A1515-A1518 (1964).

[58] M.H. Lee, Phys. Rev. E **55** (2), 1518-1520 (1997).

[59] R. K. Pathria, Phys. Rev. E **57** (3), 2697-2702 (1998).

[60] H. Saygin and A. Sisman, J. Appl. Phys. **90**, (6) 3086 (2001).

[61] Altug Sisman and Hasan Saygin, Applied Energy **68** 367-376 (2001).

[62] G. Martinez, arXiv:1304.1452.

[63] F. Karsch, *Lattice QCD at High Temperature and Density* in Lecture Notes of Physics, vol. 583, 2002. arXiv:hep-lat/0106019.

[64] J. Beringer *et al.*, Phys. Rev. D **86** (1), 010001 (2012).

[65] H. Blas and B. M. Pimentel, and J. L. Tomazelli, Phys. Rev. E **60** (5), 6164- 6167 (1999).

[66] Abramowitz and Stegun: Handbook of Mathematical Functions.

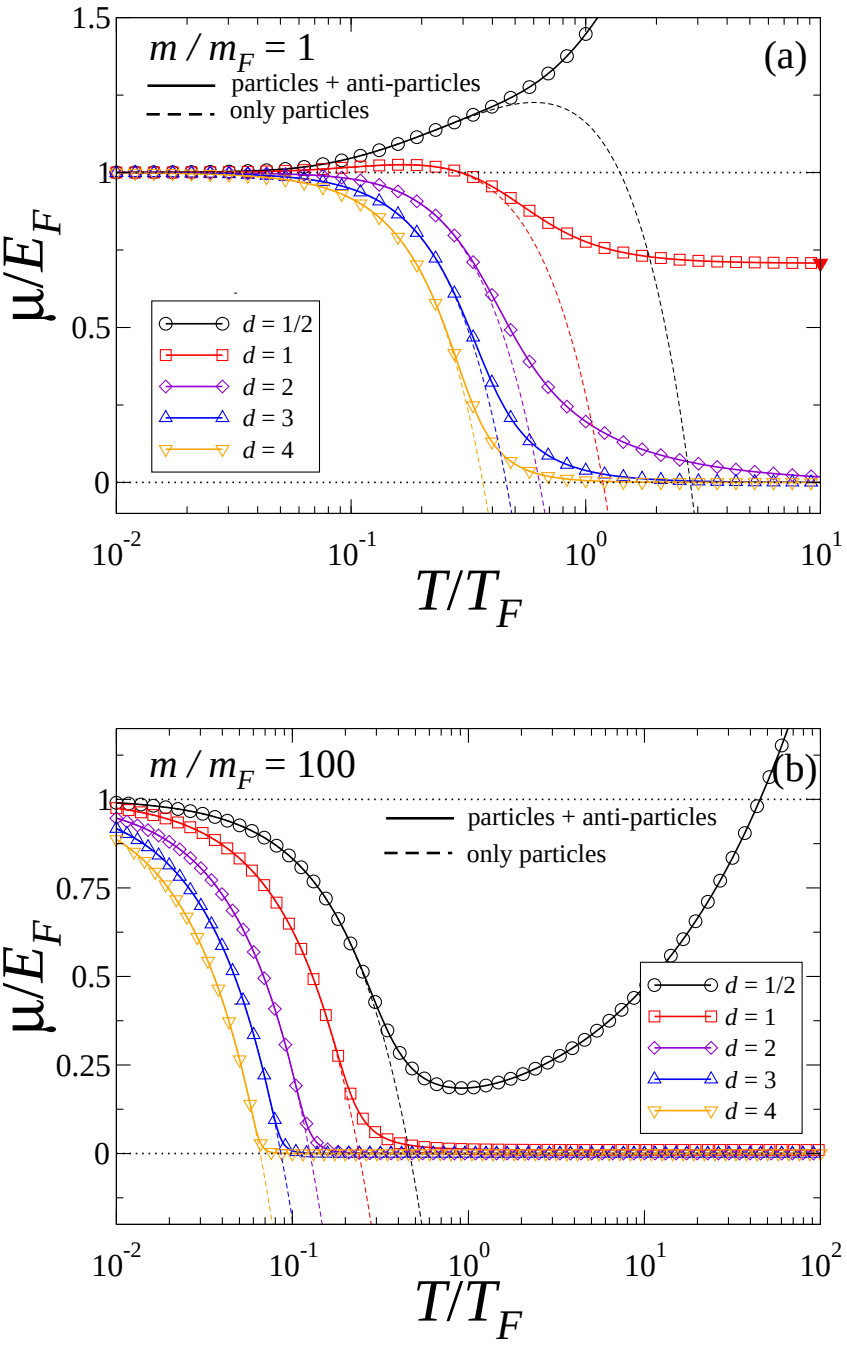

Figure 1: (Color online) Dimensionless chemical potential as function of the dimensionless temperature T/T_F, for different dimensions: 1/2 (circles), 1 (squares), 2 (diamonds), 3 (up-triangles) and 4 (down-triangles). Panel (a), (b), corresponds to $\widetilde{m} = 1$, 100, respectively. To exhibit the effects of pair production, the curves of $\mu(T, V_d)$ for the case when only particles are present in the system are also shown (dashed lines). The solid-red triangle in panel (a) gives the value $1/\sqrt{2}$ which corresponds to the asymptotic value given by expression (14) for $d = 1$.

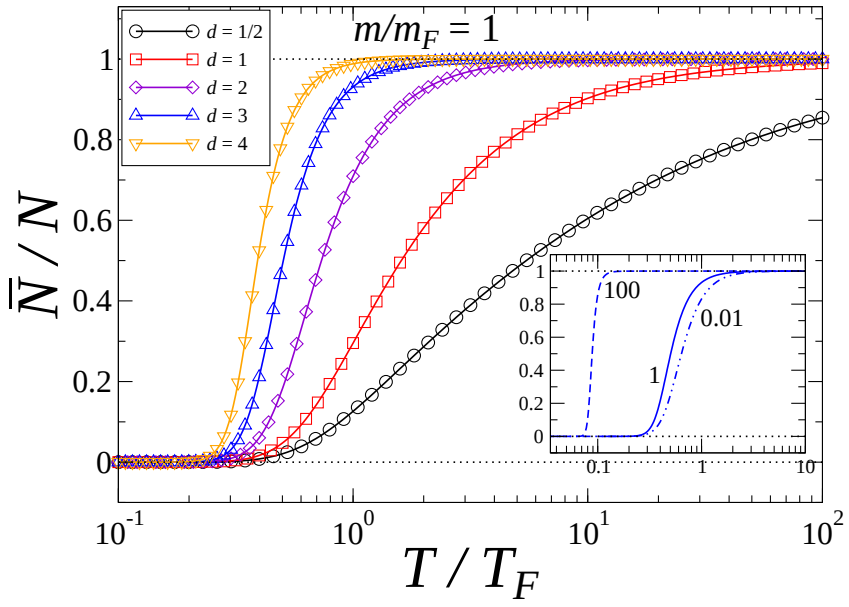

Figure 2: (Color online) Ratio of anti-particles number to the particle number as function of T/T_F for dimension 1/2 (circles), 1 (squares), 2 (diamonds), 3 (up-triangles) and 4 (down-triangles). Inset correspond to the three-dimensional case for the mass ratio values $\widetilde{m} = 0.01$ (dashed-dotted line), 1 (continuous line) and 100 (dashed line).

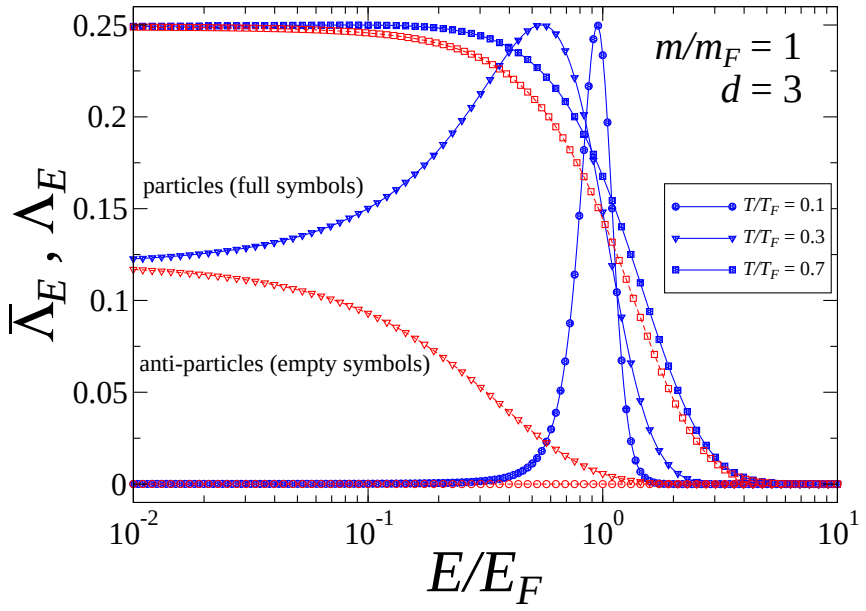

Figure 3: (Color online) $\Lambda_E, \overline{\Lambda}_E$ (as defined in text) *vs* the normalized energy E/E_F are shown for the three-dimensional relativistic IFG and for different temperatures, namely $T/T_F = 0.1$ at which pair production is negligible (circles); $T/T_F = 0.3$ when pair production starts rising (triangles); and $T/T_F = 0.7$ where antiparticles almost equals the particles number (squares).

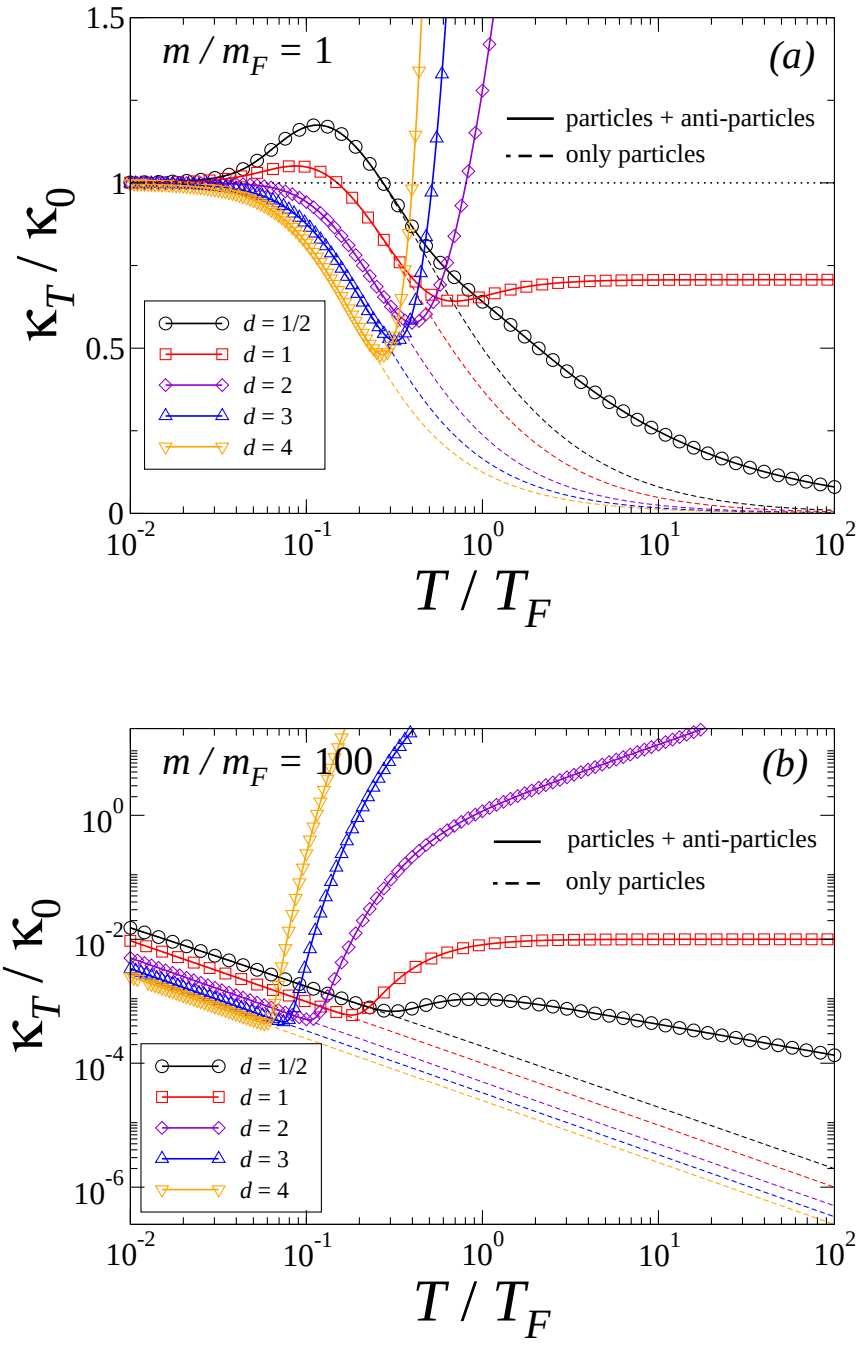

Figure 4: (Color online) Isothermal compressibility κ_T normalized with its value a $T = 0$ as function of the dimensionless temperature T/T_F and dimension 1/2 (circles), 1 (squares), 2 (diamonds), 3 (up-triangles) and 4 (down-triangles) for the mass ratio $\widetilde{m} = 1$ [panel (a)] and $\widetilde{m} = 100$ [panel (b)]. Thin-dashed lines correspond to the cases for which pair production is neglected.

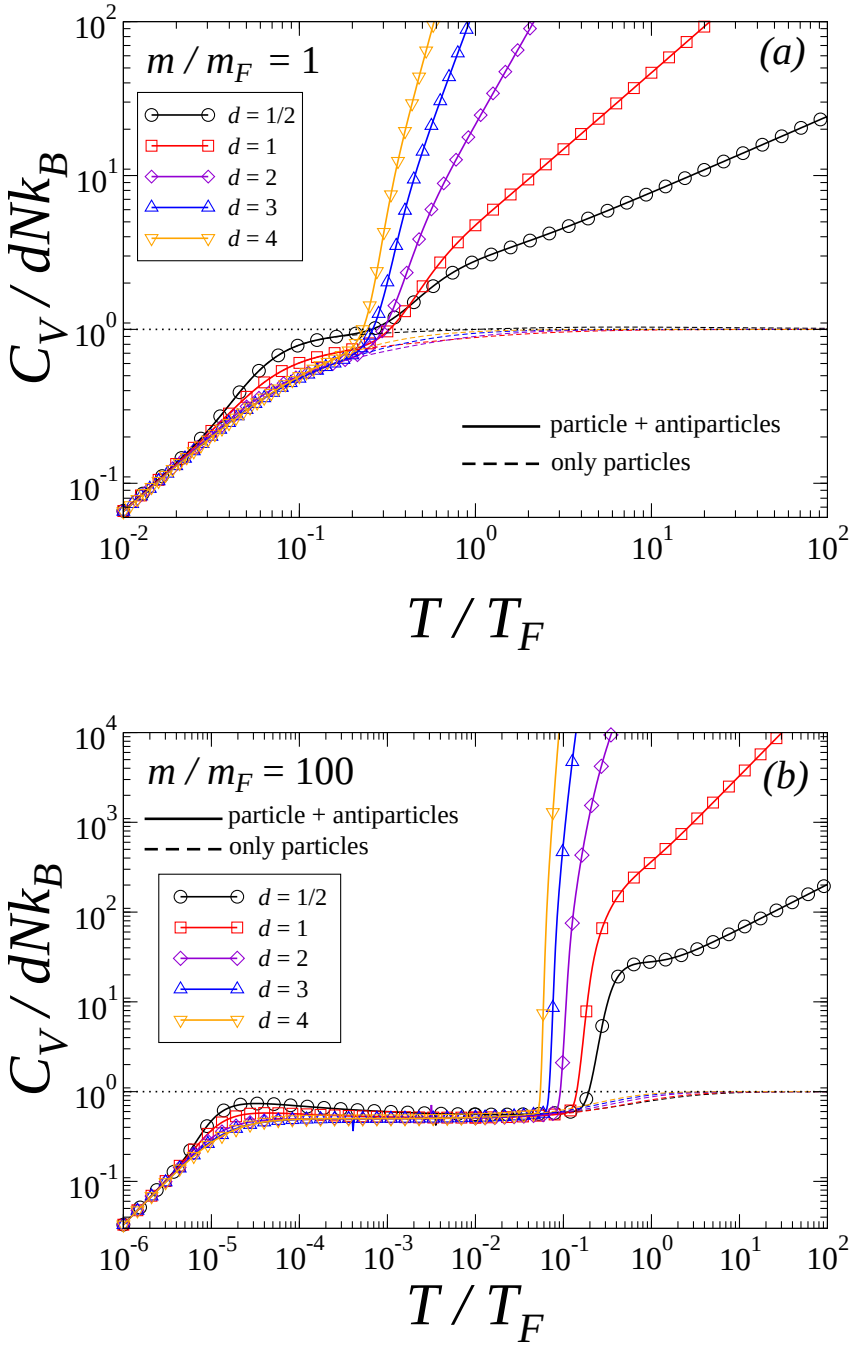

Figure 5: (Color online) Dimensionless specific heat at constant volume as function of the dimensionless temperature T/T_F for dimension 1/2 (circles), 1 (squares), 2 (diamonds), 3 (up-triangles) and 4 (down-triangles) and mass ratio $\widetilde{m} = 1$ [panel (a)], $\widetilde{m} = 100$ [panel (b)]. Thin-dashed lines correspond to the cases for which pair production is neglected.